

---

# DSAC: Distributional Soft Actor Critic for Risk-Sensitive Reinforcement Learning

---

**Xiaoteng Ma**

Tsinghua University  
ma-xt17@mails.tsinghua.edu.cn

**Li Xia\***

Sun Yat-Sen University  
xiali5@sysu.edu.cn

**Zhengyuan Zhou**

New York University  
zyzhou@stanford.edu

**Jun Yang\***

Tsinghua University  
yangjun603@tsinghua.edu.cn

**Qianchuan Zhao**

Tsinghua University  
zhaoqc@tsinghua.edu.cn

## Abstract

In this paper, we present a new reinforcement learning (RL) algorithm called Distributional Soft Actor Critic (DSAC), which exploits the distributional information of accumulated rewards to achieve better performance. Seamlessly integrating SAC (which uses entropy to encourage exploration) with a principled distributional view of the underlying objective, DSAC takes into consideration the randomness in both action and rewards, and beats the state-of-the-art baselines in several continuous control benchmarks. Moreover, with the distributional information of rewards, we propose a unified framework for risk-sensitive learning, one that goes beyond maximizing only expected accumulated rewards. Under this framework we discuss three specific risk-related metrics: percentile, mean-variance and distorted expectation. Our extensive experiments demonstrate that with distribution modeling in RL, the agent performs better for both risk-averse and risk-seeking control tasks.

## 1 Introduction

In the past few years, model-free deep reinforcement learning [Sutton and Barto, 2018, François-Lavet et al., 2018] has emerged to be an important and powerful paradigm that has been increasingly applied in several application domains [Mnih et al., 2013, Silver et al., 2016, Gu et al., 2017, Haarnoja et al., 2018a]. Such well-founded optimism stems from the large performance gains that can be potentially unlocked by using deep neural networks for function approximation in RL—either to parameterize value functions or policies—so as to harness the representation power therefrom brought forth. However, simply throwing in "deep function approximators" is far from sufficient, and building efficient and effective RL algorithms often requires sophisticated thought, one that integrates function approximation well with the unique aspects of RL.

One important such aspect is exploration: since current actions influence the future state and hence the future rewards of the underlying Markov decision process [Puterman, 1994, Bertsekas, 1995], effective exploration is a key aspect of RL algorithms. In the flourishing literature that has been developed for model-free RL, randomness in action space is widely employed as a primitive to balance exploration and exploitation. On-policy algorithms, such as A3C [Mnih et al., 2016], TRPO [Schulman et al., 2015] and PPO [Schulman et al., 2017], use stochastic action space and optimize the parameters by policy gradient. However, on-policy algorithms are not data-efficient as they require new experience for policy evaluation. On the other hand, off-policy methods can reuse past experience and hence improve data efficiency. However, most off-policy methods, such

---

\*Corresponding author.

as DQN [Mnih et al., 2015], DDPG [Van Hasselt et al., 2016] and TD3 [Fujimoto et al., 2018], inherit the simple  $\epsilon$ -greedy strategy from Q-learning by adding a small noise to a deterministic policy for exploration, where the scale of action perturbation is hard to choose in practice. To improve robustness of off-policy methods, SVG [Heess et al., 2015] introduces re-parameterized stochastic policy, while its objective is still standard maximum expected discounted returns.

Recently, Haarnoja et al. [2018b] take a principled approach for encouraging the randomness (and hence diversity) of actions by formally formulating the entropy of a policy into the objective. This maximum entropy approach is founded on theoretical principles and has been applied to many other contexts as well, such as from inverse reinforcement learning [Ziebart et al., 2008, Zhou et al., 2018] and optimal control [Todorov, 2008, Rawlik et al., 2013]. Haarnoja et al. [2018b] propose a novel continuous action space algorithm called soft actor-critic (SAC), which is more robust than former methods and has achieved the state-of-the-art performance in many continuous action control tasks. More specifically, SAC computes an optimal policy by minimizing the KL-divergence between the action distribution and the exponential form of the soft action-value function. From the view of probabilistic graphical models, the objective function of maximum entropy RL can be derived by minimizing the KL-divergence between experience distribution of the current policy and the optimal path distribution [Levine, 2018].

Concurrently, randomness in RL has been harnessed in other ways to improve performance. In particular, distributional RL [Jaquette et al., 1973, Sobel, 1982, White, 1988, Morimura et al., 2010, Bellemare et al., 2017], another approach that has gained momentum recently, proposes to take into account the whole distribution of value functions, rather than just the expectation. Since the whole distribution contains much more information beyond the first moment, one can leverage it to make more informed decisions that ultimately lead to superior rewards. Incidentally, latest experiments show that similar encouraging mechanisms also exist in human brains [Dabney et al., 2020]. An important challenge in this approach lies in approximating the distribution of value functions well. To address this challenge, a series of recent works have studied this problem and provided progressively more effective ways to achieve the goal. Categorical DQN (C51) [Bellemare et al., 2017] uses a set of discrete fixed values to estimate possibilities and outperforms DQN in Atari 2600 games. QR-DQN [Dabney et al., 2018a] replaces fixed values with fixed possibilities, and introduced quantile regression for learning quantile values. Further, Dabney et al. [2018b] extend QR-DQN with sampled quantile fractions in IQN [2018b], which is able to approximate the full quantile function with infinite samples. To avoid random samples, FQF [Yang et al., 2019] parameterizes both the quantile values and quantile fractions, which provides a fully-parameterized tool for distribution approximation. In continuous action setting, D4PG [Barth-Maron et al., 2018] combines DDPG [Van Hasselt et al., 2016] and C51 with distributed training, showing the potential of distributional RL in continuous action tasks.

These two approaches—SAC and distributional RL—when considered together, reveal the components that each misses: SAC cannot take advantage of the information beyond the first moment of values and distributional RL does not effectively encourage the diversity of actions for efficient exploration. With the benefit of hindsight, it is natural to raise the following question: **Could randomness be exploited at a deeper level that simultaneously encourages action diversity for better exploration and leverages the distributional information of value function?** It turns out, as we show in this paper, that the answer is in the affirmative.

## 1.1 Our Contributions

Our contributions are threefold. First, we design a novel algorithm, called distributional soft actor critic (DSAC), that combines maximum entropy RL with distributional RL. DSAC can be simultaneously understood as an approach that leverages distributional information of value functions in SAC and as an approach that encourages action randomness through the entropy surrogate in distributional RL. Our algorithm consists of several aspects. We define a distributional soft Bellman operator, and use quantile regression to estimate the soft discounted return for continuous action tasks. The full architecture, together with how efficient training can be performed, is discussed in detail in Section 3.

Second, we move beyond the traditional RL objective of minimizing the sum of expected future (discounted) rewards and consider risk-sensitive learning. By adapting DSAC to this setting, we provide a unified framework that can simultaneously handle several risk functionals—percentile, mean-variance, distorted expectation among others (see Section 4 for more risk metrics and details)—that

reflect the decision maker’s varied risk preferences and learn the corresponding policies. Risk-sensitive learning is an important topic that has been explored in the literature: risk measures, such as variance [Sobel, 1982, Xia, 2016, Prashanth and Fu, 2018], CVaR [Chow et al., 2015] and CPT [Tversky and Kahneman, 1992], all involve higher moments of the underlying value distribution, which does not satisfy the Bellman equation. However, each of the prior works can only handle single risk measure and only on small scales, where our key advantage is to provide a unified framework that can perform risk-sensitive learning under various metrics on large-scale RL problems.

Third, we perform extensive experimental evaluations (Section 5), comparing our algorithm to the state-of-the-art model-free RL algorithms (on continuous state/action space). Our algorithm demonstrates superior performance in standard benchmark tasks (using MuJoCo and Box2d with OpenAI Gym) and outperforms the current best algorithm SAC, thereby pushing the frontier of the performance of model-free RL. We also perform detailed simulation experiments to demonstrate the efficacy of the proposed risk-sensitive RL framework.

## 2 Background

We consider a standard Markov decision process (MDP) modeled by the tuple  $(\mathcal{S}, \mathcal{A}, R, \mathcal{P}, \gamma)$  [Puterman, 1994], where  $\mathcal{S}$  and  $\mathcal{A}$  denote the continuous state space and continuous action space respectively,  $\mathcal{P} : \mathcal{S} \times \mathcal{S} \times \mathcal{A} \rightarrow [0, \infty)$  represents the unknown transition probability density of next state given current state and action,  $R : \mathcal{S} \times \mathcal{A} \rightarrow \mathbb{R}$  denotes the reward function and  $\gamma \in (0, 1)$  denotes the discount factor. Let policy  $\pi$  denote a mapping from each state to a probability distribution over  $\mathcal{A}$  and  $\Pi$  denote the set of policies.

Standard RL aims at maximizing the expectation of the sum of discounted rewards:

$$J(\pi) = \mathbb{E}_\pi \left[ \sum_{t=0}^{\infty} \gamma^t R(s_t, a_t) \right], \quad (1)$$

with the initial state  $s_0$  drawing from the initial distribution  $\xi$ . For a policy  $\pi \in \Pi$ , action-value function  $Q^\pi : \mathcal{S} \times \mathcal{A} \rightarrow \mathbb{R}$  is defined as follows:

$$Q^\pi(s, a) := \mathbb{E}_\pi \left[ \sum_{t=0}^{\infty} \gamma^t R(s_t, a_t) \right] \mid a_t \sim \pi(\cdot | s_t), s_{t+1} \sim \mathcal{P}(\cdot | s_t, a_t), s_0 = s, a_0 = a. \quad (2)$$

The *Bellman operator*  $\mathcal{T}^\pi$  and *Bellman optimality operator*  $\mathcal{T}^*$  are defined as

$$\begin{aligned} \mathcal{T}^\pi Q(s, a) &:= \mathbb{E} [R(s, a)] + \gamma \mathbb{E}_{\mathcal{P}, \pi} [Q(s', a')], \\ \mathcal{T}^* Q(s, a) &:= \mathbb{E} [R(s, a)] + \gamma \max_{a'} \mathbb{E}_{\mathcal{P}} [Q(s', a')]. \end{aligned} \quad (3)$$

Repeated applications of either operator from some initial  $Q^0$  converges to its fixed point  $Q^\pi$  or  $Q^*$  at a geometric rate as both operators are contractive [Bertsekas and Tsitsiklis, 1995].

### 2.1 Maximum Entropy Reinforcement Learning

Different from the standard RL, maximum entropy RL maximizes the sum of rewards while keeping the entropy of policy as large as possible. The objective function of maximum entropy RL is

$$J(\pi) = \mathbb{E}_\pi \left[ \sum_{t=0}^{\infty} \gamma^t [R(s_t, a_t) + \alpha \mathcal{H}(\pi(\cdot | s_t))] \right]. \quad (4)$$

Haarnoja et al. [2018b] proposed soft actor critic (SAC) for learning the policy in continuous action space with maximum entropy objective function. By adding entropy to the standard Bellman operator  $\mathcal{T}^\pi$ , the authors defined the *soft Bellman operator*  $\mathcal{T}_S^\pi$  as

$$\mathcal{T}_S^\pi Q(s, a) := \mathbb{E} [R(s, a)] + \gamma \mathbb{E}_{\mathcal{P}, \pi} [Q(s', a') - \alpha \log \pi(a' | s')]. \quad (5)$$

SAC proceeds by repeatedly applying soft policy evaluation, followed by soft policy improvement, until convergence occurs. Similar to the standard policy evaluation, the soft policy evaluation is

completed by repeating  $\mathcal{T}_S^\pi$ . The soft policy improvement is achieved by minimizing the Kullback-Leibler divergence between the policy distribution and exponential form of soft action-value function,

$$\pi_{\text{new}} = \arg \min_{\pi' \in \Pi} \text{D}_{\text{KL}} \left( \pi'(\cdot|s_t) \parallel \frac{\frac{1}{\alpha} \exp(Q^{\pi_{\text{old}}}(s_t, \cdot))}{\Delta^{\pi_{\text{old}}}(s_t)} \right), \quad (6)$$

where  $\Delta^{\pi_{\text{old}}}$  is the partition function that normalizes the distribution.

## 2.2 Distributional Reinforcement Learning

While maximum entropy RL takes the randomness in action space into consideration, distributional RL captures another important nature of MDP, which is the randomness in accumulated discounted returns. The objective function of distributional RL is aligned with traditional RL to maximizing the discounted return in Equation 1.

To measure the distance between value distributions,  $p$ -Wasserstein distance is introduced as

$$W_p(U, V) = \left( \int_0^1 |F_U^{-1}(\omega) - F_V^{-1}(\omega)|^p d\omega \right)^{1/p}, \quad (7)$$

where  $U, V$  are two random variables and  $F_U, F_V$  are their cumulative distribution functions (CDF) for  $p < \infty$ . Let  $\mathcal{Z}$  denote the action-value distribution space with finite moments:

$$\mathcal{Z} = \{Z : \mathcal{S} \times \mathcal{A} \rightarrow \mathcal{P}(\mathbb{R}) \mid \mathbb{E}[|Z(s, a)|^p] < \infty, \forall (s, a), p \geq 1\}. \quad (8)$$

For  $Z_1, Z_2 \in \mathcal{Z}$ , a metric  $\bar{d}_p$  over value distributions is defined as

$$\bar{d}_p(Z_1, Z_2) = \sup_{s, a} W_p(Z_1(s, a), Z_2(s, a)). \quad (9)$$

The *distributional Bellman operator*  $\mathcal{T}_D^\pi : \mathcal{Z} \rightarrow \mathcal{Z}$  is defined as

$$\mathcal{T}_D^\pi Z(s, a) \stackrel{D}{=} R(s, a) + \gamma Z(s', a') \mid s' \sim \mathcal{P}(\cdot|s, a), a' \sim \pi(\cdot|s'), \quad (10)$$

where  $U \stackrel{D}{=} V$  denotes that random variables  $U$  and  $V$  follow the same distribution. This operator is a  $\gamma$ -contraction in  $\bar{d}_p$ . While  $\mathcal{T}_D^\pi$  is no longer a contraction of any distributional metric in control setting, convergence to the optimal action-state value  $Q^*$  can still be achieved by taking expectation  $\mathbb{E}[Z]$  [Bellemare et al., 2017].

While the distributional RL has good convergence properties, approximation of value distribution is a main challenge in practice.

## 3 Distributional Soft Actor Critic

In this section, we present our algorithm Distributional Soft Actor Critic (DSAC).

### 3.1 Distributional Soft Policy Iteration

In DSAC, we optimize the policy to maximize objective function in Equation 4, aligned with maximum entropy RL. Let  $Z^\pi : \mathcal{S} \times \mathcal{A} \rightarrow \mathcal{Z}$  denote the *soft action-value distribution* of a policy  $\pi \in \Pi$ , which is defined as

$$Z^\pi(s, a) \stackrel{D}{=} \sum_{t=0}^{\infty} \gamma^t [R(s_t, a_t) - \alpha \log \pi(a_{t+1}|s_{t+1})] \mid a_t \sim \pi(\cdot|s_t), s_{t+1} \sim \mathcal{P}(\cdot|s_t, a_t), s_0 = s, a_0 = a. \quad (11)$$

Taking randomness both in reward and action into consideration, we define the *distributional soft Bellman operator*  $\mathcal{T}_{DS}^\pi$  as

$$\mathcal{T}_{DS}^\pi Z(s, a) \stackrel{D}{=} R(s, a) + \gamma [Z(s', a') - \alpha \log \pi(a'|s')] \mid s' \sim \mathcal{P}(\cdot|s, a), a' \sim \pi(\cdot|s'). \quad (12)$$

Seamlessly integrating the soft Bellman operator  $\mathcal{T}_S^\pi$  defined in Equation 5 and the distributional Bellman operator  $\mathcal{T}_D^\pi$  defined in Equation 10, this operator inherits the property of convergence from original operators.

**Lemma 1**  $\mathcal{T}_{DS}^\pi : \mathcal{Z} \rightarrow \mathcal{Z}$  is a  $\gamma$ -contraction in  $\bar{d}_p$ .

With the new defined operator, an abstract algorithm similar to soft policy iteration can be obtained, which we name *distributional soft policy iteration*. The algorithm consists of two parts: *distributional soft policy evaluation* and *distributional soft policy improvement*. For any policy  $\pi$ , soft action-value distribution  $Z^\pi$  is obtained by repeatedly applying  $\mathcal{T}_{DS}^\pi$ .

**Lemma 2 (Distributional Soft Policy Evaluation)** For any mapping  $Z^0 : \mathcal{S} \times \mathcal{A} \rightarrow \mathcal{Z}$ , we define  $Z^{k+1} = \mathcal{T}_{DS}^\pi Z^k$ . The sequence  $Z^k$  will converge to  $Z^\pi$  as  $k \rightarrow \infty$ .

With a well evaluated value distribution, policy improvement is achieved by minimizing Equation 6.

**Lemma 3 (Distributional Soft Policy Improvement)** For all  $(s, a) \in \mathcal{S} \times \mathcal{A}$ , let  $Q^\pi(s, a) = \mathbb{E}[Z^\pi(s, a)]$ . With  $\pi_{\text{old}} \in \Pi$  and  $\pi_{\text{new}}$  as the solution of problem defined in Equation 6, we have  $Q^{\pi_{\text{old}}}(s, a) \leq Q^{\pi_{\text{new}}}(s, a)$ .

By repeatedly applying distributional soft policy evaluation and distributional soft policy improvement, the policy will finally converge to the optimum. See Appendix A for proofs of above lemmas.

### 3.2 The DSAC Algorithm

DSAC has an Actor-Critic network structure, which contains a distributional soft value network  $Z_\tau(s, a; \theta)$  as the critic and a stochastic policy network  $\pi(a|s; \phi)$  as the actor. We first discuss how to train the critic.

Let  $F_Z^{-1}$  denote the *quantile function* [Müller, 1997] for random variable  $Z$ , which represents the inverse function of the CDF  $F_Z(z) = Pr(Z < z)$ . By definition we have  $F_Z^{-1}(\tau) := \inf\{z \in \mathbb{R} : \tau \leq F_Z(z)\}$ , where  $\tau$  denotes the quantile fraction. In the rest, we denote  $Z_\tau := F_Z^{-1}(\tau)$ .

Given state  $s$  and action  $a$ , the action-value distribution is approximated by a number of quantile values at quantile fractions. Let  $\{\tau_i\}_{i=0, \dots, N}$  denote an ensemble of quantile fractions, which satisfy  $\tau_0 = 0, \tau_N = 1, \tau_i < \tau_j, \forall i < j$ , and  $\tau_i \in [0, 1], i = 0, \dots, N$ . We further denote  $\hat{\tau}_i = (\tau_i + \tau_{i+1})/2$ . In the literature, quantile fractions can be generated by different methods: fixed values (QR-DQN [Dabney et al., 2018a]), random sampling (IQN [Dabney et al., 2018b]) and trainable proposal network (FQF [Yang et al., 2019]). In DSAC, we do not limit which method to use, but treat the generation of quantile fractions as an independent module.

Based on Equation 12, the pairwise temporal difference (TD) error between two quantile fractions  $\hat{\tau}_i$  and  $\hat{\tau}_j$  is defined as

$$\delta_{ij}^t = r_t + \gamma [Z_{\hat{\tau}_i}(s_{t+1}, a_{t+1}; \bar{\theta}) - \alpha \log \pi(a_{t+1}|s_{t+1}; \bar{\phi})] - Z_{\hat{\tau}_j}(s_t, a_t; \theta), \quad (13)$$

where  $\bar{\theta}$  and  $\bar{\phi}$  are parameters of target action-value distribution network and target policy. The targets networks are soft-updated towards current networks for training stability.

We adopt quantile regression to train  $Z_\tau(s, a; \theta)$  by minimizing the weighted pairwise Huber regression loss of different quantile fractions. The Huber quantile regression loss [Huber, 1964] with threshold  $\kappa$  is defined as,

$$\rho_\tau^\kappa(\delta_{ij}) = |\tau - \mathbb{I}\{\delta_{ij} < 0\}| \frac{\mathcal{L}_\kappa(\delta_{ij})}{\kappa}, \text{ with } \mathcal{L}_\kappa(\delta_{ij}) = \begin{cases} \frac{1}{2} \delta_{ij}^2, & \text{if } |\delta_{ij}| \leq \kappa \\ \kappa (|\delta_{ij}| - \frac{1}{2} \kappa), & \text{otherwise.} \end{cases} \quad (14)$$

Thus the objective of quantile value network  $Z_\tau(s, a; \theta)$  is given by

$$J_Z(\theta) = \sum_{i=0}^{N-1} \sum_{j=0}^{N-1} (\tau_{i+1} - \tau_i) \rho_{\hat{\tau}_j}^\kappa(\delta_{ij}^t), \quad (15)$$

where each  $\rho_{\hat{\tau}_j}^\kappa$  is weighted by the target distribution fractions  $\tau_{i+1} - \tau_i$ .

Off-policy continuous action RL algorithms suffer from overestimation problem in calculating the target value. Double learning suggests to overcome the overestimation with two action-value functions [Fujimoto et al., 2018]. We extend the idea of double learning in TD3 to DSAC. Two same

structure networks parameterized by  $\theta_k, k = 1, 2$  are trained by fitting a same conservative target. For two quantile fractions  $\hat{\tau}_i$  and  $\hat{\tau}_j$ , the TD-error is redefined by

$$\begin{aligned} y_i^t &= \min_{k=1,2} Z_{\hat{\tau}_i}(s_{t+1}, a_{t+1}; \bar{\theta}_k), \\ \delta_{ij}^{t,k} &= r_t + \gamma (y_i^t - \alpha \log \pi(a_{t+1}|s_{t+1}; \bar{\phi})) - Z_{\hat{\tau}_j}(s_{t+1}, a_{t+1}; \theta_k). \end{aligned} \quad (16)$$

With the parameterized quantile function, it is easy to adapt SAC to train the policy network  $\pi(a|s; \phi)$ . The action-value function is obtained by taking expectation as

$$Q(s, a; \theta) = \sum_{i=0}^{N-1} (\tau_{i+1} - \tau_i) Z_{\hat{\tau}_i}(s, a; \theta). \quad (17)$$

In double variant DSAC,  $Q(s, a; \theta) = \min_{k=1,2} Q(s, a; \theta_k)$ . To solve the minimization problem in Equation 6, SAC samples action with a re-parameterized policy neural network  $f(s, \epsilon; \phi)$ , where  $\epsilon$  is a noise vector sampled from any fixed distribution, like standard spherical Gaussian. Thus the original problem can be solved by gradient descent with objective:

$$J_\pi(\phi) = \mathbb{E}_{s_t \sim \mathcal{D}, \epsilon_t \sim \mathcal{N}} [\log \pi(f(s_t, \epsilon_t; \phi) | s_t) - Q(s_t, f(s_t, \epsilon_t; \phi); \theta)], \quad (18)$$

where  $\mathcal{D}$  is the transitions replay buffer. See the complete algorithm flow in Appendix C.

## 4 A Risk-sensitive RL Framework

The distribution of returns contains more information than the expectation, which allows us to consider different risk metrics. In this section, we extend the basic DSAC to risk-sensitive RL settings and present a unified framework in which most common risk metrics can be optimized. We then discuss three specific risk measures: percentile, mean-variance and distorted expectation.

### 4.1 Policy Learning under Risk Measures

Though risk-sensitive RL is widely explored in the literature [Shen et al., 2014, Chow et al., 2015, Prashanth and Fu, 2018], most of the risk measures are hard to estimated directly as they lose the linearity of the expectation in Bellman’s equation [Puterman, 1994]. Moreover, the estimation methods of risk-related measures are often limited in small scales and tabular cases. Distributional RL provides a new perspective for optimizing policy under different risk appetites within a unified framework. With distribution of returns, it is able to approximate value function under risk measure.

Let define a *risk measure function*  $\Psi : \mathcal{Z} \rightarrow \mathbb{R}$ , which represents a mapping from the value distribution space to a real number. The *risk soft action-value* is defined as

$$Q_r(s, a) = \Psi[Z(s, a)], \quad (19)$$

where  $Z(s, a)$  is the soft action-value distribution defined in Equation 11. Thus the expectation of the soft action-value distribution can be viewed as a risk-neutral measure function with  $\Psi[\cdot] = \mathbb{E}[\cdot]$ . Note that since we take the risk measure over soft action-value distribution which contains not only reward but also entropy of policy, we change the original meaning of risk measures.

Below, we list most common risk measures to explain how to optimize them with risk related DSAC.

**Percentile** Percentile risk measure is focus on the tail of reward distribution [Filar et al., 1995]. *Value-at-risk* (VaR) are the most popular risk metric for percentile, which measures risk as the minimum reward (maximum cost) that might be incurred with respect to a given confidence level [Chow et al., 2015, Prashanth and Fu, 2018]. For a random variable  $Z$  with the CDF  $F_Z(z)$  and a confidence level  $\beta \in [0, 1]$ ,  $\text{VaR}_\beta(Z) = \min_z \{z | F_Z(z) > \beta\}$ . It is natural to approximate risk soft action-value of VaR with  $Q_r(s, a) = Z_\beta(s, a; \theta)$ , which is the estimated quantile value at a given quantile fraction  $\beta$ .

**Mean-Variance** Variance-related metric is another important risk metric [Sobel, 1982, Castro et al., 2012, Prashanth and Ghavamzadeh, 2016]. Containing the higher moment information, variance is an intuitive measure of uncertainty, fluctuation, fairness and robustness of decision. Existing

methods of variance estimation learn both the first and second moment of the discounted returns. As Bellemare et al. [2017] pointed, distributional Bellman operator  $\mathcal{T}_D^\pi$  is a contraction in variance, which means convergence in the value distribution space also leads to a good estimation of variance. We approximate variance as  $Q_v(s, a) = \sum_{i=0}^{N-1} (\tau_{i+1} - \tau_i) [Z_{\hat{\tau}_i}(s, a; \theta) - Q(s, a)]^2$ , where  $Q(s, a)$  is the expectation.

In this paper, we consider to optimize a mean-variance objective  $\Psi(Z) = \mathbb{E}[Z] - \beta\sqrt{\mathbb{V}[Z]}$ , which is a trade-off between mean and standard deviation. To be specific, we estimate this objective with  $Q_r(s, a) = Q(s, a) - \beta\sqrt{Q_v(s, a)}$ .

**Distorted Expectation** Distorted expectation is a risk weighted expectation of value distribution under a specific distortion function [Hardy, 2002, Balbás et al., 2009]. By saying a *distortion function*, we mean a non-decreasing function  $g : [0, 1] \rightarrow [0, 1]$  satisfying  $g(0) = 0$  and  $g(1) = 1$ . The *distorted expectation* of  $Z$  under  $g$  is defined as  $\Psi(Z) = \int_0^1 F_Z^{-1}(\tau) dg(\tau) = \int_0^1 g'(\tau) F_Z^{-1}(\tau) d\tau$ . By the definition, it is clear shown that expectation is distorted by  $g'(\tau)$ , and naturally the distorted action-value can be estimated by  $Q_r(s, a) = \sum_{i=0}^{N-1} (\tau_{i+1} - \tau_i) g'(\hat{\tau}_i) Z_{\hat{\tau}_i}(s, a; \theta)$ .

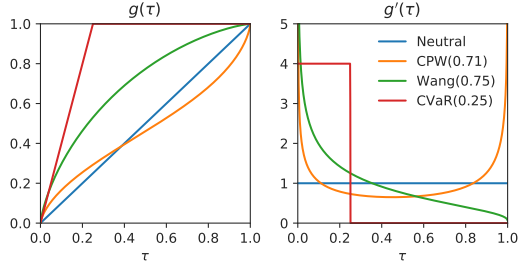


Figure 1: Different distortion functions and their derivations.

Different distortion functions reflect different risk preferences. We list some common distortion functions as follow:

- **CPW** Cumulative probability weighting parameterization:  $g(\tau) = \tau^\beta / (\tau^\beta + (1 - \tau)^\beta)^{\frac{1}{\beta}}$ . It was proposed in cumulative prospect theory [Tversky and Kahneman, 1992]. CPW is sensitive near two ends when  $\tau \rightarrow 0$  or  $\tau \rightarrow 1$ , which is similar to human decision makers. Tversky and Kahneman [1992] found  $\beta = 0.71$  matches most closely human subjects.
- **Wang** A distortion risk measure proposed by Wang [2000]:  $g(\tau) = \Phi(\Phi^{-1}(\tau) + \beta)$ , where  $\Phi$  and  $\Phi^{-1}$  are the standard Normal CDF and its inverse,  $\beta > 0$  for risk-averse and  $\beta < 0$  for risk-seeking.
- **CVaR** *Conditional Value at Risk* (CVaR) is a conditional version of VaR, which is interested in the expectation of the tail of the reward distribution. Corresponding distortion function is defined as  $g(\tau) = \min\{\tau/\beta, 1\}$ , where  $\beta \in (0, 1)$  denotes confidence level. Estimating CVaR is hard and data-inefficient, as only  $\beta$  of data could affect value of CVaR.

## 5 Experiments

To evaluate our algorithm performance, we design a series of experiments to compare DSAC with current state of the art for continuous control RL algorithms and test DSAC in different risk scenarios. We implement our algorithm based on *rlkit* [Pong et al., 2019], a well-developed PyTorch [Paszke et al., 2019] RL toolkit. All experiments are performed on NVIDIA GeForce RTX 2080 Ti 11GB graphics cards. Hyper-parameters and implementation details are listed in Appendix B.2. The source code of our DSAC implementation<sup>1</sup> is available online.

### 5.1 Comparison with State-of-the-art

We evaluate our algorithm with MuJoCo [Todorov et al., 2012] and Box2d in OpenAI Gym [Brockman et al., 2016]. First, we conduct a modular experiment to find the best way of quantile fraction generation, the result of which is shown in Appendix B.1. Comparing with fix quantiles [Dabney et al., 2018a] and a trainable network [Yang et al., 2019], random sampling [Dabney et al., 2018b] has better performance and fewer parameters. Thus we use random sampled quantile fractions in the following experiments.

<sup>1</sup><https://github.com/xtma/dsac>

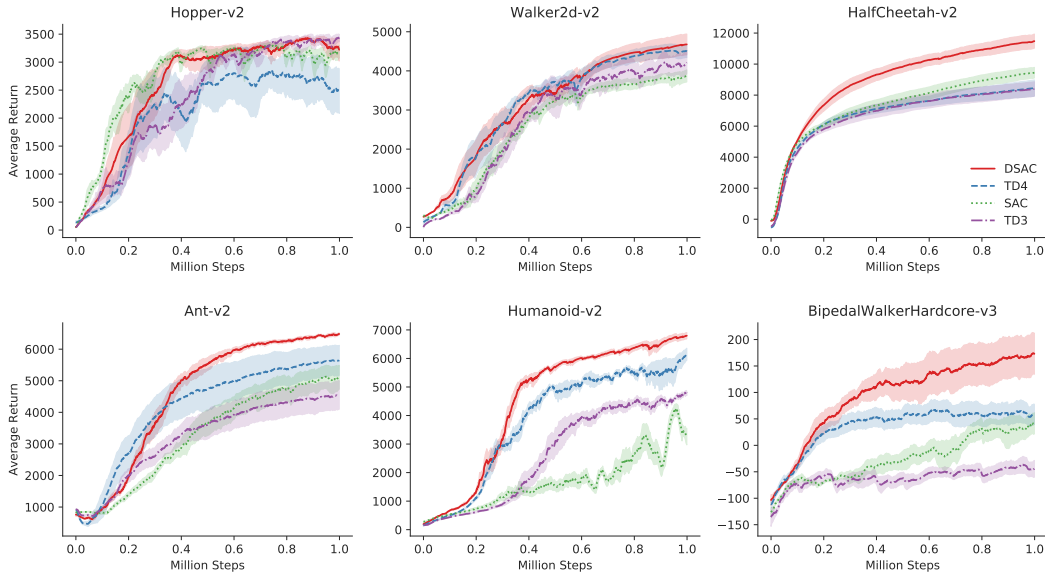


Figure 2: Learning curves for the continuous control benchmarks in MuJoCo and Box2d. Each learning curve is averaged over 5 different random seeds and shaded by the half of their variance. All curves are smoothed for better visibility.

We compare with two state-of-the-art baselines for continuous control tasks: twin delayed deep deterministic policy gradient (TD3) [Fujimoto et al., 2018] and soft actor critic (SAC) [Haarnoja et al., 2018b]. To test whether entropy of policy is effective with distributional RL, we also implement a distributional variant TD3 named twin delayed deep distributional deterministic policy gradient (TD4), which replaces the  $Q$ -network with the  $Z$ -network of DSAC while excluding entropy information in training.

The results in Figure 2 show that DSAC outperforms other baselines. Moreover, in complex tasks like *Humanoid* (which has a 17-dimensional action space) and *BipedalWalkerHardcore* (hard for exploration), DSAC has significant advantages against other methods. It needs to be pointed out that, unlike former solutions combining evolution strategy [Hämäläinen et al., 2018], implementing recurrent policy [Song et al., 2018] or using specific tricks, DSAC finishes *BipedalWalkerHardcore* with an ideal score without any targeted changes. The results illustrate the effectiveness of modeling distributional information of both reward and action.

## 5.2 Risk-averse Policies

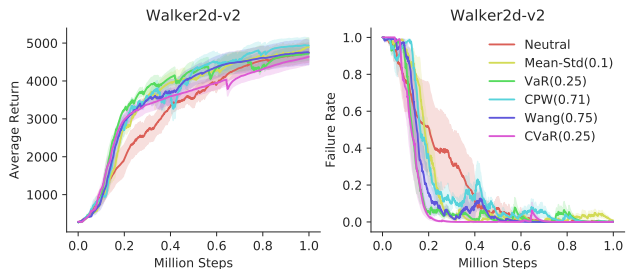


Figure 3: Comparison of different risk-averse policies. Each curve is averaged over 5 seeds.

To evaluate how the risk-averse measures affect the performance of agents, we select a set of tasks in MuJoCo, in which the robot may fall before the time runs out. In addition to the average return, we introduce failure rate to measure their performances under risk. The failure rate is calculated by the number of episodes in which the agent falls divided by the total number of evaluation. The result of *Walker2d* is shown in Figure 3 and the others are shown in Appendix D.1.

As we expected, risk-averse policies decrease the probability of falling down. However, not all the risk-measures lead to higher average scores. For example, CVaR has lowest failure rate but worst in average return. It shows introducing risk-related metric in training indeed makes a trade-off between rewards and risks, which is decisive in many safety-critical systems.



### 5.3 Risk-seeking Policies

We evaluate risk-seeking policies on *BidepalWalkerHardcore*, which is a harder variant of *BidepalWalker*. The bipedal robot agent needs to learn not only how to walk forward, but also how to jump over obstacles. We have remarked that DSAC beats other baselines in *BidepalWalkerHardcore*, moreover, risk-seeking policies can do better in such a difficult task.

We run each experiments 6 times and select top 3 random seeds to see whether risk-seeking metrics lead to higher best scores. The results, plotted in Figure 4, show risk-seeking policies outperform the risk neutral policy and achieve higher scores in the end. The improvement mainly comes from stronger exploration capability. Though distributional RL has studied to enhance exploration capability of policy in former work [Tang and Agrawal, 2018], we point out that stronger exploration capability can be obtained by introducing risk-seeking strategies.

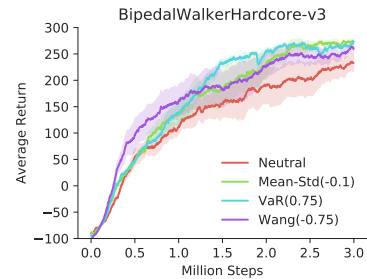


Figure 4: Comparison of different risk-seeking policies in BipedalWalkerHardcore. Each curve is averaged over top 3 seeds of 6 random seeds.

### Broader Impact

Encoding risk appetites in policy training, DSAC has a great application potential in risk-critical areas. Many risk-sensitive systems have naturally defined risk metrics, like CVaR and Sharpe Ratio [Sharpe, 1994] in finance systems. Moreover, risk measures can be understood in different ways. Many queuing systems require a balance between the average waiting time and fairness [Aviitzhak and Levy, 2004]. Performance criteria like fairness are also within the risk range discussed by DSAC. In the renewable energy systems, power fluctuations have a negative impact on the power quality of local grids [Blavette et al., 2014]. Uncertainty of renewable power can be modeled by risk metrics, like variance.

### References

- Richard S. Sutton and Andrew G. Barto. *Reinforcement learning: An introduction, Second Edition*. MIT press, 2018.
- Vincent François-Lavet, Peter Henderson, Riashat Islam, Marc G. Bellemare, Joelle Pineau, et al. An introduction to deep reinforcement learning. *Foundations and Trends® in Machine Learning*, 11(3-4):219–354, 2018.
- Volodymyr Mnih, Koray Kavukcuoglu, David Silver, Alex Graves Ioannis Antonoglou, Daan Wierstra, and Martin Riedmiller. Playing atari with deep reinforcement learning. *arXiv preprint arXiv:1312.5602*, 2013.
- David Silver, Aja Huang, Chris J Maddison, Arthur Guez, Laurent Sifre, George Van Den Driessche, Julian Schrittwieser, Ioannis Antonoglou, Veda Panneershelvam, Marc Lanctot, et al. Mastering the game of go with deep neural networks and tree search. *nature*, 529(7587):484, 2016.
- Shixiang Gu, Ethan Holly, Timothy Lillicrap, and Sergey Levine. Deep reinforcement learning for robotic manipulation with asynchronous off-policy updates. In *2017 IEEE international conference on robotics and automation (ICRA)*, pages 3389–3396. IEEE, 2017.
- Tuomas Haarnoja, Aurick Zhou, Kristian Hartikainen, George Tucker, Sehoon Ha, Jie Tan, Vikash Kumar, Henry Zhu, Abhishek Gupta, Pieter Abbeel, et al. Soft actor-critic algorithms and applications. *arXiv preprint arXiv:1812.05905*, 2018a.
- Martin L. Puterman. *Markov Decision Processes: Discrete Stochastic Dynamic Programming*. John Wiley & Sons, Inc., 1994.
- Dimitri P. Bertsekas. *Dynamic programming and optimal control*. 1995.

- Volodymyr Mnih, Adria Puigdomenech Badia, Mehdi Mirza, Alex Graves, Timothy Lillicrap, Tim Harley, David Silver, and Koray Kavukcuoglu. Asynchronous methods for deep reinforcement learning. In *International conference on machine learning*, pages 1928–1937, 2016.
- John Schulman, Sergey Levine, Pieter Abbeel, Michael Jordan, and Philipp Moritz. Trust region policy optimization. In *International conference on machine learning*, pages 1889–1897, 2015.
- John Schulman, Filip Wolski, Prafulla Dhariwal, Alec Radford, and Oleg Klimov. Proximal policy optimization algorithms. *arXiv preprint arXiv:1707.06347*, 2017.
- Volodymyr Mnih, Koray Kavukcuoglu, David Silver, Andrei A. Rusu, Joel Veness, Marc G. Belle-mare, Alex Graves, Martin Riedmiller, Andreas K. Fidjeland, Georg Ostrovski, et al. Human-level control through deep reinforcement learning. *Nature*, 518(7540):529, 2015.
- Hado Van Hasselt, Arthur Guez, and David Silver. Deep reinforcement learning with double q-learning. In *Thirtieth AAAI conference on artificial intelligence*, 2016.
- Scott Fujimoto, Herke Hoof, and David Meger. Addressing function approximation error in actor-critic methods. In *International Conference on Machine Learning*, pages 1582–1591, 2018.
- Nicolas Heess, Gregory Wayne, David Silver, Timothy Lillicrap, Tom Erez, and Yuval Tassa. Learning continuous control policies by stochastic value gradients. In *Advances in Neural Information Processing Systems*, pages 2944–2952, 2015.
- Tuomas Haarnoja, Aurick Zhou, Pieter Abbeel, and Sergey Levine. Soft actor-critic: Off-policy maximum entropy deep reinforcement learning with a stochastic actor. In *International Conference on Machine Learning*, pages 1856–1865, 2018b.
- Brian D. Ziebart, Andrew L. Maas, J. Andrew Bagnell, and Anind K. Dey. Maximum entropy inverse reinforcement learning. In *Proceedings of the Twenty-Third AAAI Conference on Artificial Intelligence, AAAI 2008, Chicago, Illinois, USA, July 13-17, 2008*, 2008.
- Zhengyuan Zhou, M Bloem, and N Bambos. Infinite time horizon maximum causal entropy inverse reinforcement learning. *IEEE Transactions on Automatic Control*, 63(9):2787–2802, 2018.
- Emanuel Todorov. General duality between optimal control and estimation. In *2008 47th IEEE Conference on Decision and Control*, pages 4286–4292. IEEE, 2008.
- Konrad Rawlik, Marc Toussaint, and Sethu Vijayakumar. On stochastic optimal control and reinforcement learning by approximate inference. In *Twenty-Third International Joint Conference on Artificial Intelligence*, 2013.
- Sergey Levine. Reinforcement learning and control as probabilistic inference: Tutorial and review. *arXiv preprint arXiv:1805.00909*, 2018.
- Stratton C. Jaquette et al. Markov decision processes with a new optimality criterion: Discrete time. *The Annals of Statistics*, 1(3):496–505, 1973.
- Matthew J. Sobel. The variance of discounted markov decision processes. *Journal of Applied Probability*, 19(4):794–802, 1982.
- D. J. White. Mean, variance, and probabilistic criteria in finite markov decision processes: a review. *Journal of Optimization Theory and Applications*, 56(1):1–29, 1988.
- Tetsuro Morimura, Masashi Sugiyama, Hisashi Kashima, Hirotaka Hachiya, and Toshiyuki Tanaka. Nonparametric return distribution approximation for reinforcement learning. In *Proceedings of the 27th International Conference on Machine Learning (ICML-10)*, pages 799–806, 2010.
- Marc G Bellemare, Will Dabney, and Rémi Munos. A distributional perspective on reinforcement learning. In *Proceedings of the 34th International Conference on Machine Learning-Volume 70*, pages 449–458. JMLR. org, 2017.
- Will Dabney, Zeb Kurth-Nelson, Naoshige Uchida, Clara Kwon Starkweather, Demis Hassabis, Rémi Munos, and Matthew Botvinick. A distributional code for value in dopamine-based reinforcement learning. *Nature*, pages 1–5, 2020.

- Will Dabney, Mark Rowland, Marc G Bellemare, and Rémi Munos. Distributional reinforcement learning with quantile regression. In *Thirty-Second AAAI Conference on Artificial Intelligence*, 2018a.
- Will Dabney, Georg Ostrovski, David Silver, and Remi Munos. Implicit quantile networks for distributional reinforcement learning. In *International Conference on Machine Learning*, pages 1104–1113, 2018b.
- Derek Yang, Li Zhao, Zichuan Lin, Tao Qin, Jiang Bian, and Tie-Yan Liu. Fully parameterized quantile function for distributional reinforcement learning. In *Advances in Neural Information Processing Systems*, pages 6190–6199, 2019.
- Gabriel Barth-Maron, Matthew W Hoffman, David Budden, Will Dabney, Dan Horgan, Alistair Muldal, Nicolas Heess, and Timothy Lillicrap. Distributed distributional deterministic policy gradients. *arXiv preprint arXiv:1804.08617*, 2018.
- Li Xia. Optimization of markov decision processes under the variance criterion. *Automatica*, 73: 269–278, 2016.
- L. A. Prashanth and Michael Fu. Risk-sensitive reinforcement learning: A constrained optimization viewpoint. *arXiv preprint arXiv:1810.09126*, 2018.
- Yinlam Chow, Aviv Tamar, Shie Mannor, and Marco Pavone. Risk-sensitive and robust decision-making: a CVaR optimization approach. In *Advances in Neural Information Processing Systems*, pages 1522–1530, 2015.
- Amos Tversky and Daniel Kahneman. Advances in prospect theory: Cumulative representation of uncertainty. *Journal of Risk and uncertainty*, 5(4):297–323, 1992.
- Dimitri P. Bertsekas and John N. Tsitsiklis. Neuro-dynamic programming: an overview. In *Proceedings of 1995 34th IEEE Conference on Decision and Control*, volume 1, pages 560–564. IEEE, 1995.
- Alfred Müller. Integral probability metrics and their generating classes of functions. *Advances in Applied Probability*, 29(2):429–443, 1997.
- Peter J. Huber. Robust estimation of a location parameter. *Annals of Mathematical Statistics*, 35(1): 492–518, 1964.
- Yun Shen, Michael J. Tobia, Tobias Sommer, and Klaus Obermayer. Risk-sensitive reinforcement learning. *Neural Computation*, 26(7):1298–1328, 2014.
- Jerzy A. Filar, Dmitry Krass, and Keith W. Ross. Percentile performance criteria for limiting average markov decision processes. *IEEE Transactions on Automatic Control*, 40(1):2–10, 1995.
- Dotan Di Castro, Aviv Tamar, and Shie Mannor. Policy gradients with variance related risk criteria. *arXiv: Learning*, 2012.
- L. A. Prashanth and Mohammad Ghavamzadeh. Variance-constrained actor-critic algorithms for discounted and average reward mdps. *Machine Learning*, 105(3):367–417, 2016.
- Mary R. Hardy. Distortion risk measures : Coherence and stochastic dominance. 2002.
- Alejandro Balbás, José Garrido, and Silvia Mayoral. Properties of distortion risk measures. *Methodology and Computing in Applied Probability*, 11(3):385, 2009.
- Shaun S. Wang. A class of distortion operators for pricing financial and insurance risks. *Journal of risk and insurance*, 67(1):15–36, 2000.
- Vitchyr Pong, M Dalal, S Lin, and A Nair. RLkit: Reinforcement learning framework and algorithms implemented in PyTorch, 2019. URL <https://github.com/vitchyr/rlkit>.
- Adam Paszke, Sam Gross, Francisco Massa, Adam Lerer, James Bradbury, Gregory Chanan, Trevor Killeen, Zeming Lin, Natalia Gimelshein, Luca Antiga, et al. PyTorch: An imperative style, high-performance deep learning library. In *Advances in Neural Information Processing Systems*, pages 8024–8035, 2019.

- Emanuel Todorov, Tom Erez, and Yuval Tassa. Mujoco: A physics engine for model-based control. In *Intelligent Robots and Systems (IROS), 2012 IEEE/RSJ International Conference on*, 2012.
- Greg Brockman, Vicki Cheung, Ludwig Pettersson, Jonas Schneider, John Schulman, Jie Tang, and Wojciech Zaremba. Openai gym. *arXiv preprint arXiv:1606.01540*, 2016.
- Perttu Hämmäläinen, Amin Babadi, Xiaoxiao Ma, and Jaakko Lehtinen. Ppo-cma: proximal policy optimization with covariance matrix adaptation. *arXiv preprint arXiv:1810.02541*, 2018.
- Doo Re Song, Chuanyu Yang, Christopher McGreavy, and Zhibin Li. Recurrent deterministic policy gradient method for bipedal locomotion on rough terrain challenge. In *2018 15th International Conference on Control, Automation, Robotics and Vision (ICARCV)*, pages 311–318. IEEE, 2018.
- Yunhao Tang and Shipra Agrawal. Exploration by distributional reinforcement learning. In *Proceedings of the 27th International Joint Conference on Artificial Intelligence*, pages 2710–2716. AAAI Press, 2018.
- William F. Sharpe. The sharpe ratio. *The Journal of Portfolio Management*, 21(1):49–58, 1994.
- Benjamin Aviitzhak and Hanoch Levy. On measuring fairness in queues. *Advances in Applied Probability*, 36(3):919–936, 2004.
- Anne Blavette, Dara Osullivan, Raymond Alcorn, Tony Lewis, and M G Egan. Impact of a medium-size wave farm on grids of different strength levels. *IEEE Transactions on Power Systems*, 29(2): 917–923, 2014.
- Geoffrey E. Hinton Jimmy Lei Ba, Jamie Ryan Kiros. Layer normalization. *arXiv preprint arXiv:1607.06450*, 2016.

## A Proof

### A.1 Lemma 1

**Lemma 1**  $\mathcal{T}_{DS}^\pi : \mathcal{Z} \rightarrow \mathcal{Z}$  is a  $\gamma$ -contraction in  $\bar{d}_p$ .

*Proof.* This lemma can be proved based on the definitions of  $\gamma$ -contraction mapping and the operator  $\mathcal{T}_{DS}^\pi$  Bellemare et al. [2017]. Let  $Z_1, Z_2 \in \mathcal{Z}$  denote two action-value distributions. For any  $(s, a) \in \mathcal{S} \times \mathcal{A}$ , we have

$$\begin{aligned} & W_p(\mathcal{T}_{DS}^\pi Z_1(s, a), \mathcal{T}_{DS}^\pi Z_2(s, a)) \\ &= W_p\left(R(s, a) + \gamma(Z_1(s, a) - \alpha \log \pi(a'|s')), \right. \\ &\quad \left. R(s, a) + \gamma(Z_2(s, a) - \alpha \log \pi(a'|s'))\right) \mid s' \sim \mathcal{P}(\cdot|s, a), a' \sim \pi(\cdot|s') \quad (20) \\ &\leq \gamma W_p(Z_1(s', a'), Z_2(s', a')) \\ &\leq \gamma \sup_{s', a'} W_p(Z_1(s', a'), Z_2(s', a')) \end{aligned}$$

By definition of  $\bar{d}_p$ , we have

$$\begin{aligned} \bar{d}_p(\mathcal{T}_{DS}^\pi Z_1, \mathcal{T}_{DS}^\pi Z_2) &= \sup_{s, a} W_p(\mathcal{T}_{DS}^\pi Z_1(s, a), \mathcal{T}_{DS}^\pi Z_2(s, a)) \\ &\leq \gamma \sup_{s', a'} W_p(Z_1(s', a'), Z_2(s', a')) \quad (21) \\ &= \gamma \bar{d}_p(Z_1, Z_2) \end{aligned}$$

### A.2 Lemma 2

**Lemma 2 (Distributional Soft Policy Evaluation)** For any mapping  $Z^0 : \mathcal{S} \times \mathcal{A} \rightarrow \mathcal{Z}$ , we define  $Z^{k+1} = \mathcal{T}_{DS}^\pi Z^k$ . The sequence  $Z^k$  will converge to  $Z^\pi$  as  $k \rightarrow \infty$ .

*Proof.* As we have proved that  $\mathcal{T}_{DS}^\pi$  is a  $\gamma$ -contraction, policy evaluation can be obtained by repeatedly applying  $\mathcal{T}_{DS}^\pi$ .

### A.3 Lemma 3

**Lemma 3 (Distributional Soft Policy Improvement)** For all  $(s, a) \in \mathcal{S} \times \mathcal{A}$ , let  $Q^\pi(s, a) = \mathbb{E}[Z^\pi(s, a)]$ . With  $\pi_{\text{old}} \in \Pi$  and  $\pi_{\text{new}}$  as the solution of problem defined in Equation 6, we have  $Q^{\pi_{\text{old}}}(s, a) \leq Q^{\pi_{\text{new}}}(s, a)$ .

*Proof.* The proof of this lemma has the similar idea to that of the soft policy improvement in [Haarnoja et al., 2018b].

For any policy  $\pi \in \Pi$  and its soft action-value distribution  $Z^\pi$ , we define the soft action-value by taking the expectation,

$$Q^\pi(s, a) = \mathbb{E}[Z^\pi(s, a)] = \mathbb{E}[R(s, a)] + \gamma \mathbb{E}_{s' \sim \mathcal{P}(\cdot|s, a), a' \sim \pi(\cdot|s')} [Z^\pi(s', a') - \alpha \log \pi(a'|s')]. \quad (22)$$

Let denote a policy  $\pi_{\text{old}} \in \Pi$  and its soft action-value  $Q^{\pi_{\text{old}}}$ . We can obtain a new policy  $\pi_{\text{new}} \in \Pi$  by solving the minimization problem defined in Equation 6,

$$\pi_{\text{new}}(\cdot|s) = \arg \min_{\pi' \in \Pi} \text{D}_{\text{KL}} \left( \pi'(\cdot|s) \parallel \exp \left( \frac{1}{\alpha} Q^{\pi_{\text{old}}}(s, \cdot) - \log \Delta^{\pi_{\text{old}}}(s) \right) \right). \quad (23)$$

Since  $\pi_{\text{new}}$  is the solution to the minimization problem above, it must be

$$\begin{aligned} & \mathbb{E}_{a \sim \pi_{\text{new}}(\cdot|s)} \left[ \log \pi_{\text{new}}(a|s) - \frac{1}{\alpha} Q^{\pi_{\text{old}}}(s, a) + \log \Delta^{\pi_{\text{old}}}(s) \right] \\ & \leq \mathbb{E}_{a \sim \pi_{\text{old}}(\cdot|s)} \left[ \log \pi_{\text{old}}(a|s) - \frac{1}{\alpha} Q^{\pi_{\text{old}}}(s, a) + \log \Delta^{\pi_{\text{old}}}(s) \right], \quad (24) \end{aligned}$$

which can be reduced as follows for partition function  $\log \Delta^{\pi_{\text{old}}}$  is only related to  $s$ ,

$$\mathbb{E}_{a \sim \pi_{\text{new}}(\cdot|s)} [\alpha \log \pi_{\text{new}}(a|s) - Q^{\pi_{\text{old}}}(s, a)] \leq \mathbb{E}_{a \sim \pi_{\text{old}}(\cdot|s)} [\alpha \log \pi_{\text{old}}(a|s) - Q^{\pi_{\text{old}}}(s, a)]. \quad (25)$$

Thus, we expand the soft Bellman equation and have

$$\begin{aligned} Q^{\pi_{\text{old}}}(s_t, a_t) &= \mathbb{E}[R(s_t, a_t)] + \gamma \mathbb{E}_{\substack{s_{t+1} \sim \mathcal{P}(\cdot|s_t, a_t) \\ a_{t+1} \sim \pi_{\text{old}}(\cdot|s_{t+1})}} [Q^{\pi_{\text{old}}}(s_{t+1}, a_{t+1}) - \alpha \log \pi_{\text{old}}(a_{t+1}|s_{t+1})] \\ &\leq \mathbb{E}[R(s_t, a_t)] + \gamma \mathbb{E}_{\substack{s_{t+1} \sim \mathcal{P}(\cdot|s_t, a_t) \\ a_{t+1} \sim \pi_{\text{new}}(\cdot|s_{t+1})}} [Q^{\pi_{\text{old}}}(s_{t+1}, a_{t+1}) - \alpha \log \pi_{\text{new}}(a_{t+1}|s_{t+1})] \\ &\vdots \\ &\leq Q^{\pi_{\text{new}}}(s_t, a_t). \end{aligned} \quad (26)$$

## B Implementation Details

### B.1 Quantile fraction Generation

Many different approaches are presented for approximating the distribution in recent years. As we consider quantile regression for distribution approximation in DSAC, we adapt QR-DQN [Dabney et al., 2018a], IQN [Dabney et al., 2018b] and FQF [Yang et al., 2019] into following quantile fraction proposal methods.

**Fix** QR-DQN [Dabney et al., 2018a] first introduced quantile regression to improve the distribution approximation. By replacing the fix value atoms in C51 [Bellemare et al., 2017], the value distribution is approximated by a group of trainable quantile values at fixed quantile fractions. With the basic idea of QR-DQN, quantile fractions are given by a group of fix values as  $\tau_i = i/N, i = 0, \dots, N$ .

**Random** Dabney et al. [2018b] extended the fixed quantile fractions to uniform samples and proposed implicit quantile value network (IQN). With infinite sampled quantile fractions, IQN is able to approximate the full quantile function. IQN uniformly samples the quantile fractions and takes the expectation in training. As we fix the number of quantile fractions and keep them in ascending order, we adapt the sampling as  $\tau_0 = 0, \tau_i = \epsilon_i / \sum_{i=0}^{N-1} \epsilon_i$  where  $\epsilon_i \sim U[0, 1], i = 1, \dots, N$ .

**Net** Instead of sampling the quantile fractions uniformly, Yang et al. [2019] proposed the fully parameterized quantile function (FQF) to parameterize both the quantile values and quantile fractions. In addition to the quantile value network, FQF uses an additional fraction proposal network  $q(s, a; \omega)$ , which has a softmax output layer and cumulatively sums the outputs as quantile fractions. The gradient of  $\omega$  is given by the gradient of  $W_1$  with respect to  $\tau$ ,

$$\frac{\partial W_1}{\partial \tau_i} = 2Z_{\tau_i}(s, a; \theta) - Z_{\hat{\tau}_i}(s, a; \theta) - Z_{\hat{\tau}_{i-1}}(s, a; \theta), \quad (27)$$

where  $W_1$  denotes 1-Wasserstein error between approximated quantile function and the true quantile function.

Though we do not limit the method for quantile fraction generation, a modular experiment is provided. Three methods—fix, random and net—are evaluated on the MuJoCO and Box2d. To be specific, quantile proposal network in FQF is a two-layer 128-unit fully connected network with learning rate set as  $1e-5$ . We show the results in Figure 5. Based on the experiment results, we choose random for quantile fraction generation, as it has better performance than fix and fewer parameters than net.

### B.2 Hyper-Parameter Setting

Hyper-parameters used in experiments and environment specific parameters are listed in Table 1.

Instead of using fixed the temperature parameter  $\alpha$  to balance reward and entropy, SAC has a variant [Haarnoja et al., 2018a] which introduces a mechanism of fine-tuning  $\alpha$  to achieve target entropy adaptively. While our algorithm does not conflict with this parameter adaptive method, we use fixed  $\alpha$  suggested in original SAC paper in our experiments to reduce irrelevant factors.

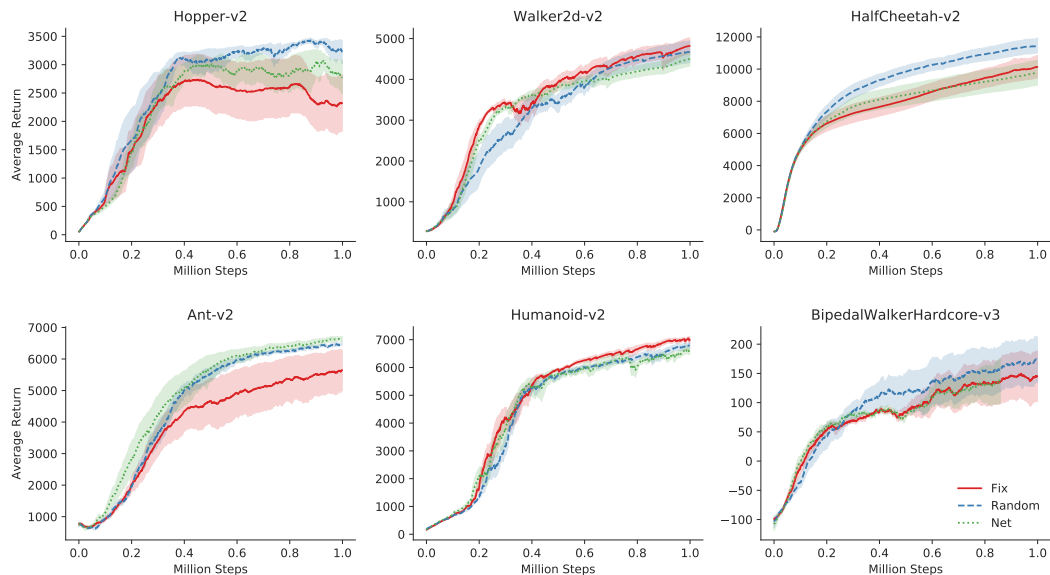


Figure 5: Comparison of quantile fraction generation methods in MuJoCo and Box2d. Each learning curve is averaged over 5 different random seeds and shaded by the half of their variance. All curves are smoothed for better visibility.

Table 1: Hyper-parameters Sheet

Hyper-parameter	Value
<i>Shared</i>	
Policy network learning rate	3e-4
(Quantile) Value network learning rate	3e-4
Optimizer	Adam
Discount factor	0.99
Target smoothing	5e-3
Batch size	256
Replay buffer size	1e6
Minimum steps before training	1e4
<i>TD3 &amp; TD4</i>	
Target policy noise	0.2
Clip target policy noise	0.5
Policy update period	2
<i>DSAC &amp; TD4</i>	
Number of quantile fractions	32
Quantile fraction embedding size	64
Huber regression threshold	1

Environment	Temperature Parameter	Max episode length
Walker2d-v2	0.2	1000
Hopper-v2	0.2	1000
Ant-v2	0.2	1000
HalfCheetah-v2	0.2	1000
Humanoid-v2	0.05	1000
BipedalWalkerHardcore-v3	0.002	2000

### B.3 Network Structure

For SAC and TD3, we utilize two-layer fully connected networks with 256 hidden units for both value and policy network and ReLU as activation function. DSAC has the same structure of policy network  $\pi_\phi(a|s; \phi)$ .

In order to embed quantile fraction  $\tau$  into the quantile value network, we borrow the idea of implicit representations from IQN [Dabney et al., 2018b]. With the element-wise (Hadamard) product (denoted as  $\odot$ ) of state feature  $\psi(s, a)$  and embedding  $\varphi(\tau)$ , the quantile values are given by  $Z_\tau(s, a) = Z(\psi(s, a) \odot \varphi(\tau); \theta)$ . After studying different ways for embedding  $\tau$ , IQN suggests an embedding formula with  $\cos(\cdot)$ ,

$$\varphi_j(\tau) := f\left(\sum_{i=1}^n \cos(i\pi\tau)w_{ij} + b_j\right), \tag{28}$$

where  $w_{ij}, b_j$  are network parameters, and  $f$  is the nonlinear activation function which is ReLU in IQN and FQF. However, in our practice, we find that using the activate function ReLU will make training unstable as the activation values  $\psi \odot \varphi$  may contain too many zeros after multiplication. Therefore, we replace ReLU in Equation 28 with Sigmoid keeping the activation values more meaningful.

We use one-layer 256-unit fully connected network for  $\psi(s, a)$  and one-layer 64-unit fully connected network for  $\varphi(\tau)$  in Equation 28, followed with one-layer 256-unit fully connected network for their multiplied values  $\psi(s, a) \odot \varphi(\tau)$ . Moreover, since magnitudes of quantile values vary hugely, we implement layer normalization [Jimmy Lei Ba, 2016] to the hidden activation of quantile value network. To help understanding the structure of our quantile value network  $Z_\tau(s, a|\theta)$ , we give a PyTorch [Paszke et al., 2019] implementation.



```

import numpy as np
import torch
from torch import nn as nn

class QuantileValueNet(nn.Module):

    def __init__(
        self,
        input_size, # state_dim + action_dim
        hidden_size=256,
        embedding_size=64,
        num_quantiles=32,
    ):
        super().__init__()
        self.num_quantiles = num_quantiles
        self.embedding_size = embedding_size
        self.psi_fc = nn.Sequential(
            nn.Linear(input_size, hidden_size),
            nn.LayerNorm(hidden_size),
            nn.ReLU(),
        )
        self.phi_fc = nn.Sequential(
            nn.Linear(embedding_size, hidden_size),
            nn.LayerNorm(hidden_size),
            nn.Sigmoid(),
        )
        self.merge_fc = nn.Sequential(
            nn.Linear(hidden_size, hidden_size),
            nn.LayerNorm(hidden_size),
            nn.ReLU(),
        )
        self.last_fc = nn.Linear(hidden_size, 1)
        self.const_vec = torch.range(1, 1 + self.embedding_size)

    def forward(self, state, action, tau):
        """
        Calculate Quantile Value in Batch
        tau: quantile fractions, (N, T)
        """
        h = torch.cat([state, action], dim=1)
        h = self.psi_fc(h) # (N, C)

        x = torch.cos(tau.unsqueeze(-1) * self.const_vec * np.pi)
        x = self.phi_fc(x) # (N, T, C)

        h = torch.mul(x, h.unsqueeze(-2)) # (N, T, C)
        h = self.merge_fc(h) # (N, T, C)
        output = self.last_fc(h).squeeze(-1) # (N, T)
        return output

```

## C Algorithm

---

### Algorithm 1 DSAC update

---

**Parameter:**  $N, \kappa$   
**Input:**  $s, a, r, s', \gamma \in (0, 1)$   
 Generate quantile fractions  $\tau_i, i = 0, \dots, N, \tau_j, j = 0, \dots, N$   
 # Update Quantile Value Network  $Z(s, a; \theta_k)$   
 Get next actions for calculating target  $a' \sim \pi(\cdot | s'; \bar{\phi})$   
**for**  $i = 0$  **to**  $N - 1$  **do**  
   **for**  $j = 0$  **to**  $N - 1$  **do**  
      $y_i = \min_{k=1,2} Z_{\hat{\tau}_i}(s', a'; \bar{\theta}_k)$   
      $\delta_{ij}^k = r + \gamma [y_i - \alpha \log \pi(a' | s'; \bar{\phi})] - Z_{\hat{\tau}_j}(s, a; \theta_k), k = 1, 2$   
   **end for**  
**end for**  
 $J_Z(\theta_k) = \frac{1}{N} \sum_{i=0}^{N-1} \sum_{j=0}^{N-1} (\tau_{i+1} - \tau_i) \rho_{\hat{\tau}_j}^\kappa(\delta_{ij}^k), k = 1, 2$   
 Update  $\theta_k$  with  $\nabla J_Z(\theta_k), k = 1, 2$   
 Update  $\bar{\theta}_k \leftarrow \iota \theta_k + (1 - \iota) \bar{\theta}_k, k = 1, 2$   
 # Update Policy Network  $\pi(a | s; \phi)$   
 Get new actions with re-parameterized samples  $\tilde{a} \sim \pi(\cdot | s; \phi)$   
 $Q(s, \tilde{a}) = \sum_{i=0}^{N-1} (\tau_{i+1} - \tau_i) \min_{k=1,2} Z_{\hat{\tau}_i}(s, \tilde{a}; \theta_k)$   
 $J_\pi(\phi) = \log(\pi(\tilde{a} | s; \phi)) - Q(s, \tilde{a})$   
 Update  $\phi$  with  $\nabla J_\pi(\phi)$   
 Update  $\bar{\phi} \leftarrow \iota \phi + (1 - \iota) \bar{\phi}$

---

## D Additional Results

We compare different risk-averse policies on 4 selected MuJoCo tasks: *Hopper*, *Walker2d*, *Ant* and *Humanoid*. Among all risk-averse measures, CVaR has the lowest failure rates in most tasks as it is most related to falls.

### D.1 Risk-averse policies on MuJoCo

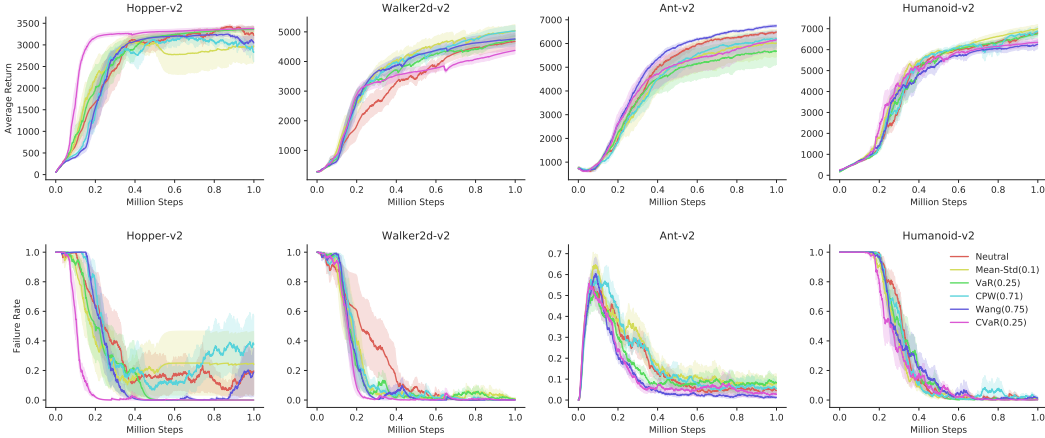


Figure 6: Comparison of different risk-averse policies. Each curve is averaged over 5 seeds.